

Universal scaling in BCS superconductivity in three dimensions in non- s waves*

Angsula Ghosh and Sadhan K. Adhikari
 Instituto de Física Teórica, Universidade Estadual Paulista
 01.405-900 São Paulo, São Paulo, Brazil

February 1, 2008

Abstract

The solutions of a renormalized BCS equation are studied in three space dimensions in s , p and d waves for finite-range separable potentials in the weak to medium coupling region. In the weak-coupling limit, the present BCS model yields a small coherence length ξ and a large critical temperature, T_c , appropriate for some high- T_c materials. The BCS gap, T_c , ξ and specific heat $C_s(T_c)$ as a function of zero-temperature condensation energy are found to exhibit potential-independent universal scalings. The entropy, specific heat, spin susceptibility and penetration depth as a function of temperature exhibit universal scaling below T_c in p and d waves.

PACS Numbers: 74.20.Fg, 74.72.-h

1 Introduction

At low temperature, a collection of weakly interacting electrons spontaneously form large overlapping Cooper pairs [1] according to the microscopic Bardeen-Cooper-Schrieffer (BCS) theory of superconductivity [2, 3]. There has been renewed interest in this problem with the discovery of enhanced superconductivity in alkali-metal-fulleride compounds [4] and cuprates [5]. The fulleride compounds, with critical temperature T_c up to $\sim 30 - 40$ K, exhibit superconductivity in three dimensions and have a relatively small coherence length ξ : $\xi k_F \sim 10 - 100$, with k_F the Fermi momentum. At zero temperature ξ is essentially the pair radius. In the application of the BCS theory to high- T_c materials, the serious challenge is to consistently produce a large T_c and a small ξ in the weak-coupling region. The usual phonon-induced BCS model is unable to produce a large T_c in the weak-coupling region.

Despite much effort, the normal state of the high- T_c superconductors has not been satisfactorily understood. Unlike the conventional superconductors, their normal state exhibits peculiar properties. The thermodynamic and electromagnetic observables of these materials above T_c have temperature dependencies which are very different from those of a Fermi liquid [6]. There

*To Appear in European Physical Journal B

are controversies about the appropriate microscopic hamiltonian, pairing mechanism, and gap parameter for them[6, 7].

The BCS theory considers N electrons of spacing L , interacting via a weak potential of short range r_0 such that $r_0 \ll L$ and $r_0 \ll \xi$. When suitably scaled, most properties of the system should be insensitive to the details of the potential and be universal functions of the dimensionless variable L/ξ [8]. In this work we study the weak-coupling BCS problem in three dimensions for s , p , and d waves with two objectives in mind. The first is to identify the universal nature of the solution appropriate to high- T_c superconductors. We would specially be interested to find out if the weak-coupling BCS theory can explain some of the universal behaviors of high- T_c materials independent of the above-mentioned controversies. The second objective is to find out to what extent the universal nature of the solution is modified in the presence of realistic finite-range (nonlocal separable) potentials. Instead of solving the BCS equation on the lattice with appropriate symmetry, we solved the equations in the continuum. This procedure should suffice for present objectives. There is also the possibility of Cooper pairing in non- s waves, such as, p -wave pairing in superfluid ^3He [9, 10] and d -wave pairing in some superconductors [5]. Hence the present discussion of universality is also extended to p and d waves.

In place of the standard phonon-induced BCS model we employ a renormalized BCS model in three dimensions with separable and zero-range potentials, which has certain advantages. The standard BCS model yields the following linear correlation between T_c and T_D , where T_D is the Debye temperature: $T_c \approx 1.13T_D \exp(-1/\bar{\lambda})$ [3], where $\bar{\lambda}$ is the effective strength of the phonon-induced BCS interaction. Due to the above correlation with T_D , T_c of the standard BCS model is low. This correlation between T_c and T_D is fundamental in explaining the observed isotope effect in conventional superconductors [3]. The high- T_c materials exhibit a very reduced and negligible isotope effect and a visible linear correlation between T_c and T_F [11], where T_F is the Fermi temperature. The present renormalized BCS model yields a linear scaling between T_c and T_F . Because of this scaling with T_F , the present T_c can be large and appropriate for the high- T_c materials in the weak-coupling region. In addition, the present model also produces an appropriate T_c/T_F ratio and a small ξ in the weak-coupling region in accord with recent experiments [11] on high- T_c materials.

Previously, there have been studies of the solution of BCS equations in terms of potential strength, V_0 , or the pair scattering length in vacuum, a , employing a short-range potential [12]. Such studies have not revealed the universal nature of the transition from weak- to medium-coupling. Here, we employ the zero-temperature condensation energy per particle, ΔU , of the BCS condensate as the reference variable for studying the problem. As ΔU increases, one passes from weak to medium coupling. We calculate the zero-temperature BCS gap $\Delta(0)$, T_c , the specific heat per particle $C_s(T_c)$ in different partial waves and the zero-temperature pair size ξ in s wave. These observables obey robust universal scaling as functions of ΔU valid over several decades in the weak-coupling region independent of the range of potential. Similar scalings were not found when $\Delta(0)$, T_c , $C_s(T_c)$ and ξ were considered as a function of V_0 or a as in Ref. [12].

We also calculate the temperature dependencies of different quantities, such as, the BCS gap $\Delta(T)$, penetration depth $\lambda_s(T)$, spin-susceptibility $\chi_s(T)$, $C_s(T)$, internal energy per particle $U_s(T)$ and entropy $S_s(T)$ for $T < T_c$. Of these, the T dependencies of $S_s(T)$, $C_s(T)$, $\chi_s(T)$, and $\lambda_s(T)$ are interesting. For isotropic s wave, the BCS theory yields exponential dependence

on temperature as $T \rightarrow 0$ for these observables independent of space dimension [3, 13]. The observed power-law dependence on temperature in some of these quantities [13, 14, 15] can be explained with anisotropic gap function in non- s waves with node(s) on the Fermi surface. We find universal power-law dependence in non- s waves independent of the range or strength of potential. For $l \neq 0$ we find

$$S_s(T)/S_s(T_c) \approx (T/T_c)^{\beta_s} \quad (1)$$

$$C_s(T)/C_n(T_c) \approx D(T/T_c)^{\beta_C} \quad (2)$$

$$\chi_s(T)/\chi_s(T_c) \approx (T/T_c)^{\beta_\chi} \quad (3)$$

$$\Delta\lambda(T) \equiv (\lambda_s(T) - \lambda_s(0))/\lambda_s(0) \sim (T/T_c)^{\beta_\lambda}, \quad (4)$$

valid for a wide range of temperature. The suffix n and s refer to normal and superconducting states, respectively. Similar power-law dependencies were predicted from an analysis of experimental data [14] as well as from a calculation based on Eliashberg equation [15].

From the weak-coupling BCS theory we established the following relations analytically: $\Delta(0)/\sqrt{\Delta U} = \sqrt{8/3}$, $T_c/\sqrt{\Delta U} = \sqrt{8/3}A^{-1}$, $G \equiv C_s(T_c)/\sqrt{\Delta U} = \sqrt{2/3}(\pi^2 A^{-1} + 1.5AB^2)$, $\xi^2 = \Delta^{-2}(0)/2 = 3/(16\Delta U)$, $H \equiv (D - 1) = \Delta C/C_n(T_c) = 1.5A^2B^2/\pi^2$, and $\Delta U/U_n(T_c) = 1.5A^2/\pi^2$ where $\Delta C = C_s(T_c) - C_n(T_c)$ and the universal constants A and B are defined by $A \equiv \Delta(0)/T_c$ and $B^2 = -[d\{\Delta(T)/\Delta(0)\}^2/d(T/T_c)]_{T=T_c}$. Unless the units of the variables are explicitly mentioned, all energy (momentum) variables are expressed in units of E_F (k_F), such that $\mu \equiv \mu/E_F$, $T \equiv T/T_F$, $q \equiv q/k_F$, $E_{\mathbf{q}} \equiv E_{\mathbf{q}}/E_F$, $E_F = k_F = k_B = 1$, etc, where μ is the chemical potential and E_F is the Fermi energy. The lengths are expressed in units of k_F^{-1} : $\xi \equiv \xi k_F$.

In Sec. II we derive the present renormalized BCS and number equations. In Sec. III we present an analytic study of the renormalized BCS equation and find several universal relations among the observables. In Sec. IV we present a numerical study of the present equation and establish power-law temperature dependence of some of the observables below T_c in non- s waves. Finally, in Sec. V we present a summary of our findings.

2 Renormalized BCS and Number Equations

We consider a weakly attractive short-range potential between electrons in the angular momentum state lm ,

$$V_{\mathbf{p}\mathbf{q}} = -V_0 g_{plm} g_{qlm} Y_{lm}(\Omega_p) Y_{lm}(\Omega_q), \quad (5)$$

where g is the potential form factor and Ω ($= \theta\phi$) represents the polar and azimuthal angles. This potential leads to Cooper instability for any V_0 and lm . In even (odd) partial waves, pairing occurs in singlet (triplet) state governed by the Cooper equation

$$V_0^{-1} = \sum_{\mathbf{q}(q>1)} g_{qlm}^2 |Y_{lm}(\Omega_q)|^2 (2\epsilon_q - \hat{E})^{-1}, \quad (6)$$

with $B_c \equiv (2 - \hat{E})$ the Cooper binding, $\epsilon_q = \hbar^2 q^2/2m$ where q is the wave number and m the electron mass.

At a finite temperature, T , one has the following BCS gap and number equations for N electrons

$$\Delta_{\mathbf{p}} = -\sum_{\mathbf{q}} V_{\mathbf{p}\mathbf{q}} \frac{\Delta_{\mathbf{q}}}{2E_{\mathbf{q}}} \tanh \frac{E_{\mathbf{q}}}{2T}, \quad (7)$$

$$N = \sum_{\mathbf{q}} \left[1 - \frac{\epsilon_{\mathbf{q}} - \mu}{E_{\mathbf{q}}} \tanh \frac{E_{\mathbf{q}}}{2T} \right], \quad (8)$$

where $E_{\mathbf{q}} = [(\epsilon_{\mathbf{q}} - \mu)^2 + |\Delta_{\mathbf{q}}|^2]^{1/2}$, with $\Delta_{\mathbf{q}}$ the gap function and μ the chemical potential. Though it is possible to have a BCS condensate in a mixed angular momentum state, here we assume, as in Ref. [10], that the condensate is formed in a state of well-defined lm , so that $\Delta_{\mathbf{q}}$ has the following anisotropic form: $\Delta_{\mathbf{q}} \equiv g_{qlm} \Delta_0 \sqrt{4\pi} Y_{lm}(\Omega_{\mathbf{q}})$ where Δ_0 and g_{qlm} are dimensionless. The BCS gap is defined by $\Delta(T) = g_{q(=1)lm} \Delta_0$, which is the root-mean-square average of $\Delta_{\mathbf{q}}$ on the Fermi surface. Equations (6) and (7) lead to the renormalized BCS equation

$$\sum_{\mathbf{q}(q>1)} \frac{|g_{qlm} Y_{lm}|^2}{2\epsilon_{\mathbf{q}} - \hat{E}} - \sum_{\mathbf{q}} \frac{|g_{qlm} Y_{lm}|^2}{2E_{\mathbf{q}}} \tanh \frac{E_{\mathbf{q}}}{2T} = 0. \quad (9)$$

The summation is evaluated according to

$$\sum_{\mathbf{q}} \rightarrow \frac{N}{4\pi} \frac{3}{4} \int_0^\infty \sqrt{\epsilon_q} d\epsilon_q \int d\Omega, \quad (10)$$

where $\int d\Omega = \int_0^{2\pi} d\phi \int_0^\pi \sin \theta d\theta$. Equations (8) and (9) can be explicitly written as

$$\int d\Omega \int d\epsilon_q \sqrt{\epsilon_q} \left[1 - \frac{\epsilon_q - \mu}{E_q} \tanh \frac{E_q}{2T} \right] = \frac{16\pi}{3}, \quad (11)$$

$$\begin{aligned} \int d\Omega |Y_{lm}|^2 & \left[\int_1^\infty d\epsilon_q \frac{\sqrt{\epsilon_q} g_{qlm}^2}{\epsilon_q - \hat{E}} - \int_0^\infty d\epsilon_q \frac{\sqrt{\epsilon_q} g_{qlm}^2}{E_q} \right. \\ & \times \left. \tanh \frac{E_q}{2T} \right] = 0. \end{aligned} \quad (12)$$

The two terms in Eq. (11) or (12) under integral have ultraviolet divergences. However, the difference between these two terms is finite. In the absence of potential form factors ($g_{qlm} = 1$), these equations are completely independent of potential and are governed by the observable B_c . This is why these equations are called renormalized BCS equations [7, 16]. The quantity B_c plays the role of a potential-independent coupling of interaction.

Now we calculate the critical temperature T_c of Eq. (12), in the special case $g_{qlm} = 1$. This potential is independent of a range parameter and is usually called a zero-range potential. At $T = T_c$, ($\Delta(T_c) = 0$), Eq. (12) can be analytically integrated to yield

$$T_c = \frac{2\exp(\gamma - 1)}{\pi} \sqrt{2B_c} \approx 0.590 \sqrt{B_c}, \quad (13)$$

where $\gamma = 0.57722\dots$ is the Euler constant. If T_F is a few thousand Kelvins, for a small B_c in the weak-coupling region, one can have $T_c > 100$ K appropriate for some high- T_c materials. The standard BCS model yields in this case [3]

$$\frac{T_c}{T_D} = \frac{\exp(\gamma)}{\pi} \sqrt{\frac{2B_c}{T_D}}. \quad (14)$$

To illustrate the advantage of Eq. (13) over (14) in predicting a large T_c in the weak-coupling limit, let us consider a specific example with $T_D = 300$ K and $T_F = 3000$ K. In the standard BCS result (14), the weak-coupling region is usually defined by $B_c \approx 1$ meV or $B_c/T_D \approx 0.037$. The smallness of B_c justifies the weak-coupling limit and we take $B_c \leq 1$ meV as defining the weak-coupling region. Schrieffer [2] suggested that B_c is the proper measure of coupling. He noted that $B_c = 0.1$ meV is safely within the weak-coupling domain. In this case for $B_c = 1$ meV $= 0.0037$ one obtains from Eq. (14) that T_c is 46 K. From Eq. (13), we obtain $T_c = 0.036 = 107$ K. This result reflects an enhancement of T_c in the renormalized model. In order to provide further evidence of the weak coupling limit of the present renormalized model with $T_c = 0.036$, we solved the number equation (11) numerically for the chemical potential μ and obtained $\mu = 1.000$, which is in the weak-coupling domain. The renormalized result (13) has the advantage of producing the experimentally observed linear scaling between T_c and T_F in high- T_c materials [11].

3 Analytic Study of the Renormalized BCS Equation

There is no cut-off in the renormalized BCS equation (12). At $T = 0$ Eq. (12) can be solved analytically in the absence of potential form factors: $g_{qlm} = 1$. Then each integral in Eq. (12) is divergent at the upper limit Λ , but for a sufficiently large Λ the difference becomes finite. Now Eq. (12) can be integrated in the weak-coupling limit ($\mu = 1$) to yield:

$$2\sqrt{\Lambda} - \ln(e^2 B_c/8) = 2\sqrt{\Lambda} - 2\ln[e^2 \Delta(0)\sqrt{4\pi}/8] + \ln F^2,$$

where $\ln F = -\int d\Omega |Y_{lm}(\Omega)|^2 \ln |Y_{lm}(\Omega)|$ with $e = 2.718281\dots$. For $\Lambda \rightarrow \infty$ this leads to $\Delta(0) = F\sqrt{2B_c}/(e\sqrt{\pi})$. However, T_c is given by Eq. (13) for all lm . In this case we have the universal constant $A \equiv \Delta(0)/T_c = F\sqrt{\pi}/\{2\exp(\gamma)\}$.

Though A is independent of interaction model and dimension of space, $\Delta(0)$ and T_c are dependent on them. For example, for a s -wave zero-range interaction we have $\Delta(0) = \sqrt{2B_c}$ and $T_c = \exp(\gamma)\sqrt{2B_c}/\pi$ from a renormalized BCS model in two dimensions[7], distinct from the above three-dimensional relations. For a fixed coupling, denoted by a B_c , we find an enhancement of T_c in two dimensions over that in three dimensions by a factor of $e/2$. In both two and three dimensions the renormalized BCS equation provides an enhanced T_c over the standard BCS T_c given by Eq. (14).

The entropy of the system is given by [3]

$$S(T) = -2 \sum_{\mathbf{q}} [(1 - f_{\mathbf{q}}) \ln(1 - f_{\mathbf{q}}) + f_{\mathbf{q}} \ln f_{\mathbf{q}}], \quad (15)$$

where $f_{\mathbf{q}} = 1/(1 + \exp(E_{\mathbf{q}}/T))$.

The condensation energy per particle at $T = 0$ is given by [3]

$$\Delta U \equiv |U_s - U_n| = \sum_{\mathbf{q}(q < 1)} 2\zeta_q - \sum_{\mathbf{q}} (\zeta_q - \frac{\zeta_q^2}{E_{\mathbf{q}}} - \frac{\Delta_{\mathbf{q}}^2}{2E_{\mathbf{q}}}),$$

where $\zeta_q = (\epsilon_q - \mu)$. In the absence of potential form factors this can be evaluated to lead to [3]

$$\Delta U = \frac{3}{8} \int d\Omega \Delta^2(0) |Y_{lm}(\Omega)|^2,$$

which yields $\Delta(0)/\sqrt{\Delta U} = \sqrt{8/3}$ for all lm . Using the universal relation between $\Delta(0)$ and T_c , one obtains $T_c/\sqrt{\Delta U} = \sqrt{8/3}A^{-1}$. For all lm , $U_n(T_c) = \pi^2 T_c^2/4$, so that $\Delta U/U_n(T_c) = 3A^2/(2\pi^2)$.

The superconducting specific heat per particle is given by

$$C_s = \frac{2}{NT^2} \sum_{\mathbf{q}} f_{\mathbf{q}}(1 - f_{\mathbf{q}}) \left(E_{\mathbf{q}}^2 - \frac{1}{2} T \frac{d\Delta_{\mathbf{q}}^2}{dT} \right). \quad (16)$$

The normal specific heat C_n is given by Eq. (16) with $\Delta_{\mathbf{q}} = 0$. The jump in specific heat per particle at $T = T_c$ ($\Delta(T_c) = 0$), $\Delta C \equiv [C_s - C_n]_{T_c}$ is given by [3]

$$\Delta C = -\frac{1}{NT_c} \sum_{\mathbf{q}} \left[f_{\mathbf{q}}(1 - f_{\mathbf{q}}) \frac{d\Delta_{\mathbf{q}}^2}{dT} \right]_{T_c}. \quad (17)$$

In the special case $g_{qlm} = 1$, the radial integral in Eq. (17) can be evaluated as in Ref. [3] and we get [3]

$$\begin{aligned} \Delta C &= -\frac{3}{4T_c} \int d\Omega \int \sqrt{\epsilon_q} d\epsilon_q \\ &\times \left[f_{\mathbf{q}}(1 - f_{\mathbf{q}}) \frac{d\Delta^2(T)}{dT} \right]_{T_c} |Y_{lm}(\Omega)|^2. \end{aligned} \quad (18)$$

This leads to [3] $\Delta C = -(3/4)[d\Delta^2(T)/dT]_{T=T_c} = (3/4)A^2B^2T_c$ for all lm . From this, we obtain $H \equiv (D - 1) = \Delta C/C_n(T_c) \equiv 1.5A^2B^2/\pi^2$, where $C_n(T_c) = \pi^2 T_c/2$, so that $C_s(T_c) = (\pi^2 + 1.5A^2B^2)T_c/2$. Consequently, $C_s(T_c)/\sqrt{\Delta U} \equiv G = \sqrt{2/3}(\pi^2 A^{-1} + 1.5AB^2)$. The numerical values of the constants A , B , H , F and G are given in Table I.

The spin-susceptibility χ of the system is defined by [10]

$$\chi(T) = \frac{2\mu_N^2}{T} \sum_{\mathbf{q}} f_{\mathbf{q}}(1 - f_{\mathbf{q}}), \quad (19)$$

where μ_N is the nuclear magneton. At $T = T_c$, $\chi_s(T) = \chi_n(T)$ and it is appropriate to study the ratio $\chi_s(T)/\chi_n(T_c)$.

Finally, it is also of interest to study the penetration depth λ defined by [3]

$$\lambda^{-2}(T) = \lambda^{-2}(0) \left[1 - \frac{2}{NT} \sum_{\mathbf{q}} f_{\mathbf{q}}(1 - f_{\mathbf{q}}) \right]. \quad (20)$$

In the numerical study of next section we shall calculate $\Delta\lambda(T) = (\lambda(T) - \lambda(0))/\lambda(0)$.

The dimensionless s -wave pair radius defined by $\xi^2 = \langle \psi_q | r^2 | \psi_q \rangle / \langle \psi_q | \psi_q \rangle$, with the pair wave function $\psi_q = g_{qlm} \Delta / (2E_q)$, can be evaluated by using $r^2 = -\nabla_q^2$. In the weak-coupling limit, the zero-range analytic result of Ref. [7] leads to $\xi^2 = \Delta^{-2}(0)/2 = 3/(16\Delta U)$. Consequently,

$$\xi = \frac{1}{\sqrt{2\Delta T_c}} \quad (21)$$

4 Numerical Study

Equations (11) and (12) are solved numerically without approximation in s , p and d waves for separable potentials with dimensionless form factors $g_{qlm} = \epsilon_q^{l/2} [\alpha / (\epsilon_q + \alpha)]^{(l+2)/2}$ with correct threshold behavior as $q \rightarrow 0$, where α is the range parameter. (Normally, one uses in Eq. (10) $d\epsilon_q \sqrt{\epsilon_q} = d\epsilon_q [2, 3]$.) Following Refs. [3, 10], we calculated $\Delta(0)$, T_c , $C_s(T_c)$, the s -wave pair radius ξ^2 at $T = 0$ as well as $\Delta(T)$, $\lambda(T)$, $C(T)$, $S(T)$, and $U(T)$ for different V_0 and α . In Fig. 1 we plot $\Delta(0)$, T_c , $C_s(T_c)$, and ξ^2 versus ΔU and establish universal scalings mentioned before. The calculations were repeated by varying α from 1 to ∞ and we found Fig. 1 to be insensitive to this variation for each lm . For $l \neq 0$, Eqs. (11) and (12) diverge for $\alpha \rightarrow \infty$ and calculations were performed for $\alpha = 1$ to 10. The increase in ΔU of Fig. 1 corresponds to an increase in coupling V_0 . We could plot the variables of Fig. 1 in terms of V_0 as in Ref. [12]. Then each α leads to a distinct curve. However, if we express the variation in V_0 by a variation of an observable of the superconductor, such as ΔU or T_c , universal potential-independent scalings are obtained. In each case the exponent and prefactor of each scaling relation are in excellent agreement with the analytic result obtained above without form factors.

TABLE I. Numerical values of various constants and exponents in different angular momentum states

lm	F	A	B	H	G	β_S \approx	β_C \approx	β_χ \approx	β_λ \approx
00	3.5449	1.764	1.74	1.43	11.11				
10	2.8563	1.422	1.60	0.79	10.12	2	2		1.1
11	3.3300	1.658	1.68	1.18	10.59	3	2.6		2.4
20	2.7748	1.382	1.57	0.72	10.00	2	2	1.2	1.1
21	3.1006	1.544	1.63	0.96	10.24	2.1	2	1.4	1.5
22	3.1006	1.544	1.63	0.96	10.24	2.1	2	1.4	1.5

The T_c should not arbitrarily increase with coupling as Fig. 1 may imply. With increased coupling the electron pairs form composite bosons which undergo Bose condensation below $T = T_c \equiv 0.218$, for bosons with twice the electron mass and half the electron density [12]. Hence the T_c curve of Fig. 1 is only plotted up to about $T_c = 0.1$. For a large class of unconventional three-dimensional superconductors T_c has been estimated to be 0.05 [11], where the universality of the present study should hold. For a typical high- T_c material $T_c = 0.04$ and from Eq. (21) we find pair-size $\xi \approx 10$ in s wave. Hence with the increase of T_c , ξ has reduced appropriately in the weak coupling region as found experimentally.

Next we studied the temperature dependence of $\Delta(T)$, $S_s(T)$, $C_s(T)$, $\chi_s(T)$, $U_s(T)$, and $\lambda_s(T)$ for $T < T_c$ for different V_0 , and range α varying from 1 to ∞ . We found that $\Delta(T)/\Delta(0)$ versus T/T_c is an universal function for each lm independent of potential parameters. We

find the universal fit $\Delta(T)/\Delta(0) \approx B(1 - T/T_c)^{1/2}$ valid for $T \approx T_c$ with numerical values of B quoted in Table I. For s -wave BCS superconductors $S_s(T)$, $C_s(T)$, $\chi_s(T)$, and $\lambda_s(T)$ have exponential dependence on T as $T \rightarrow 0$. But for non- s wave states, these variables have power-law dependence on T as observed in some materials [13, 14, 15]. In Figs. 2, 3, 4, and 5 we plot $S_s(T)/S_n(T_c)$, $C_s(T)/C_n(T_c)$, $\chi_s(T)/\chi_n(T_c)$, and $\Delta\lambda(T)/\lambda(0)$, respectively, versus T/T_c where $\Delta\lambda(T) = (\lambda(T) - \lambda(0))/\lambda(0)$. As commented in Ref. [10], χ_s will be significantly different from χ_n only for even l . We have calculated χ_s only for $l = 0$ and 2. Scalings (1) – (4) are established in Figs. 2 – 5. The exponents of these scalings are given in Table I. In order to find β_C we also plotted $C_s(T)/C_n(T_c)$ versus T/T_c on log scale. That plot was used to calculate the exponent β_C . However, on log scale different curves nearly overlap and hence that plot is not shown here. From Fig. 3 we find that the zero of $[C_s(T) - C_n(T)]$ appears in all cases for $T/T_c \approx 0.5$. Moreover, all curves for superconducting specific heat meet at $T/T_c \approx 0.6$. These two behaviors seems to be typical for models based on BCS equations.

The constants in Table I for different lm satisfy $\mathcal{C}_{00} > \mathcal{C}_{11} > \mathcal{C}_{21} = \mathcal{C}_{22} > \mathcal{C}_{10} > \mathcal{C}_{20}$, where \mathcal{C}_{lm} stands for F , A , B , H , and G . Hence the following sequence of lm states represents the increase of anisotropy for the gap function: 00, 11, (21,22), 10, and 20. From the plot of entropy in Fig. 2, we find that this sequence of lm also represents the increase of disorder and consequently, a decrease in superconductivity or an approximation to the normal state, as is clear from Figs. 3 – 5. Because of approximation to more anisotropy and disorder, the observables for the normal state are closer to the superconducting $l \neq 0$ state than to the superconducting $l = 0$ state.

The exponents β_S , β_C , β_χ and β_λ are critical exponents near $T = T_c$. Wilson [18] discussed the universal nature of similar critical exponents in ferromagnetism and concluded that the numerical value of those exponents depend on the dimensionality of space and the symmetry of the order parameter of phase transition. Recently, we have calculated some of these exponents using the renormalized BCS equation in two dimensions [17]. From these studies it seems that these universal critical exponents of BCS superconductivity are also determined by the dimensionality of space and the symmetry of the order parameter $\Delta_{\mathbf{q}}$.

5 Conclusion

Through a numerical study of the renormalized weak-coupling BCS equation in three dimensions in s , p and d waves we have established robust scaling of $\Delta(0)$, T_c , $C_s(T_c)$, and ξ^2 , as a function of ΔU , independent of range of a general separable potential. The T dependence of $S_s(T)$, $C_s(T)$, $\chi_s(T)$, and $\Delta\lambda(T)$ below T_c in non- s waves show power-law scalings distinct to some high- T_c materials [13, 14, 15]. No power-law T dependence is found in s wave for these observables. The universal nature of the solution does not essentially change with the potential range and remains valid for a zero-range potential. In the weak-coupling limit the present solutions of the renormalized BCS equations simulates typical high- T_c values for the coherence length ξ , and T_c . They also exhibit the T_c versus T_F linear correlation (at a fixed B_c) as observed by Uemura [11].

We thank John Simon Guggenheim Memorial Foundation, Conselho Nacional de Desenvolvimento Científico e Tecnológico and Fundação de Amparo à Pesquisa do Estado de São Paulo for financial support.

References

- [1] L. N. Cooper, Phys. Rev. **104**, 1189 (1956).
- [2] J. Bardeen, L. N. Cooper, and J. R. Schrieffer, Phys. Rev. **108**, 1175 (1957); J. R. Schrieffer, *Theory of Superconductivity*, (Benjamin, New York, 1964).
- [3] M. Tinkham, *Introduction to Superconductivity*, (McGraw-Hill Inc., New York, 1975).
- [4] A. F. Hebard, Phys. Today **45**, #11, 26 (1992).
- [5] B. G. Levi, Phys. Today **46**, #5, 17 (1993).
- [6] H. Ding, Nature **382**, 51 (1996); N. Trivedi and M. Randeria, Phys. Rev. Lett. **75**, 312 (1995).
- [7] M. Randeria, J-M. Duan, and L-Y. Shieh, Phys. Rev. B **41**, 327 (1990); S. K. Adhikari and A. Ghosh, *ibid.* **55**, 1110 (1997); R. M. Carter et al., *ibid.* **52**, 16149 (1995).
- [8] A. J. Leggett, J. Phys. (Paris) Colloq. **41**, C7-19 (1980).
- [9] A. J. Leggett, Rev. Mod. Phys. **47**, 331 (1975).
- [10] P. W. Anderson and P. Morel, Phys. Rev. **123**, 1911 (1961).
- [11] Y. J. Uemura *et al.*, Phys. Rev. Lett. **66**, 2665 (1991).
- [12] P. Nozières and S. Schmitt-Rink, J. Low Temp. Phys. **59**, 195 (1985).
- [13] J. Annett, N. Goldenfeld, and S. R. Renn, Phys. Rev. B **43** 2778 (1991).
- [14] K. A. Moler *et al.*, Phys. Rev. Lett. **73**, 2744 (1994); H. Hardy *et al.*, *ibid.* **70**, 3999 (1993).
- [15] M. Prohammer, A. Perez-Gonzalez, and J. P. Carbotte, Phys. Rev. B **47**, 15152 (1993).
- [16] For an account of renormalization in nonrelativistic quantum mechanics, see, for example, S. K. Adhikari and T. Frederico, Phys. Rev. Lett. **74**, 4572 (1995); S. K. Adhikari, T. Frederico, and I. D. Goldman, *ibid.* **74**, 487 (1995); S. K. Adhikari, T. Frederico, and R. M. Marinho, J. Phys. A: Math. Gen. **29**, 7157 (1996); S. K. Adhikari and A. Ghosh, *ibid.* **30**, 6553 (1997).
- [17] S. K. Adhikari and A. Ghosh, unpublished.
- [18] K. G. Wilson, Scientific American **241**, 140 (1979).

Figure Captions:

1. $C_s(T_c)$ (dashed line), T_c (dotted line), $\Delta(0)$ (dashed-dotted line) for different lm and s -wave pair radius ξ^2 (solid line) versus zero-temperature condensation energy ΔU for different V_0 and α (from 1 to ∞). For $C_s(T_c)$ and T_c there are six distinct lines and for $\Delta(0)$ we have a single line for all α and lm . The lines for $C_s(T_c)$ (T_c) correspond to $lm = 00, 11, (21, 22), 10$, and 20 from top to bottom (bottom to top).

2. Entropy $S_s(T)/S_s(T_c)$ versus T/T_c for different lm , V_0 , and α between 1 to ∞ . The curves are labelled by lm .

3. Same as Fig. 2 for specific heat $C_s(T)/C_n(T_c)$ versus T/T_c .

4. Same as Fig. 2 for spin-susceptibility $\chi_s(T)/\chi_s(T_c)$ versus T/T_c .

5. Same as Fig. 2 for $\Delta\lambda(T)$ versus T/T_c .

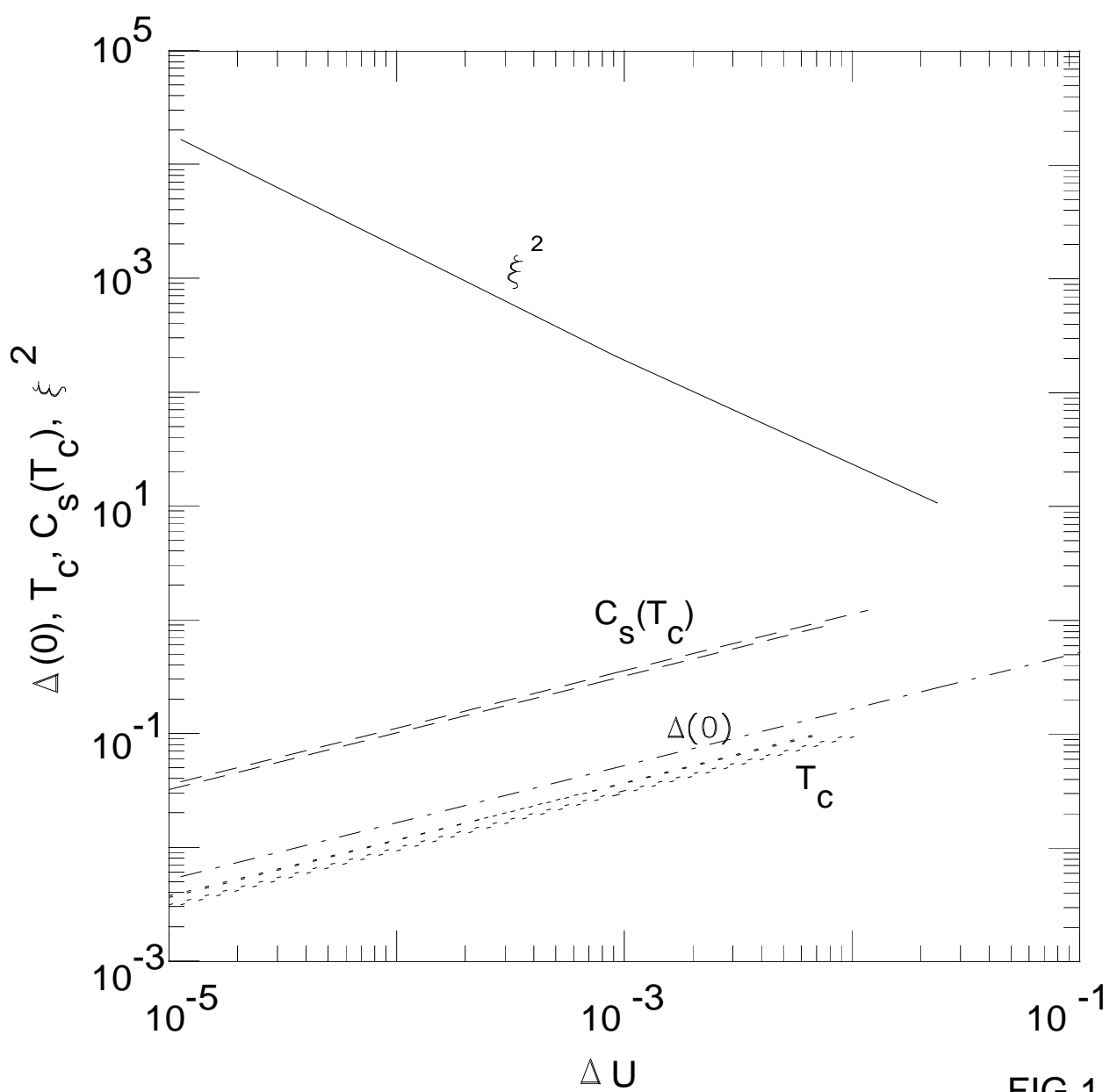


FIG 1

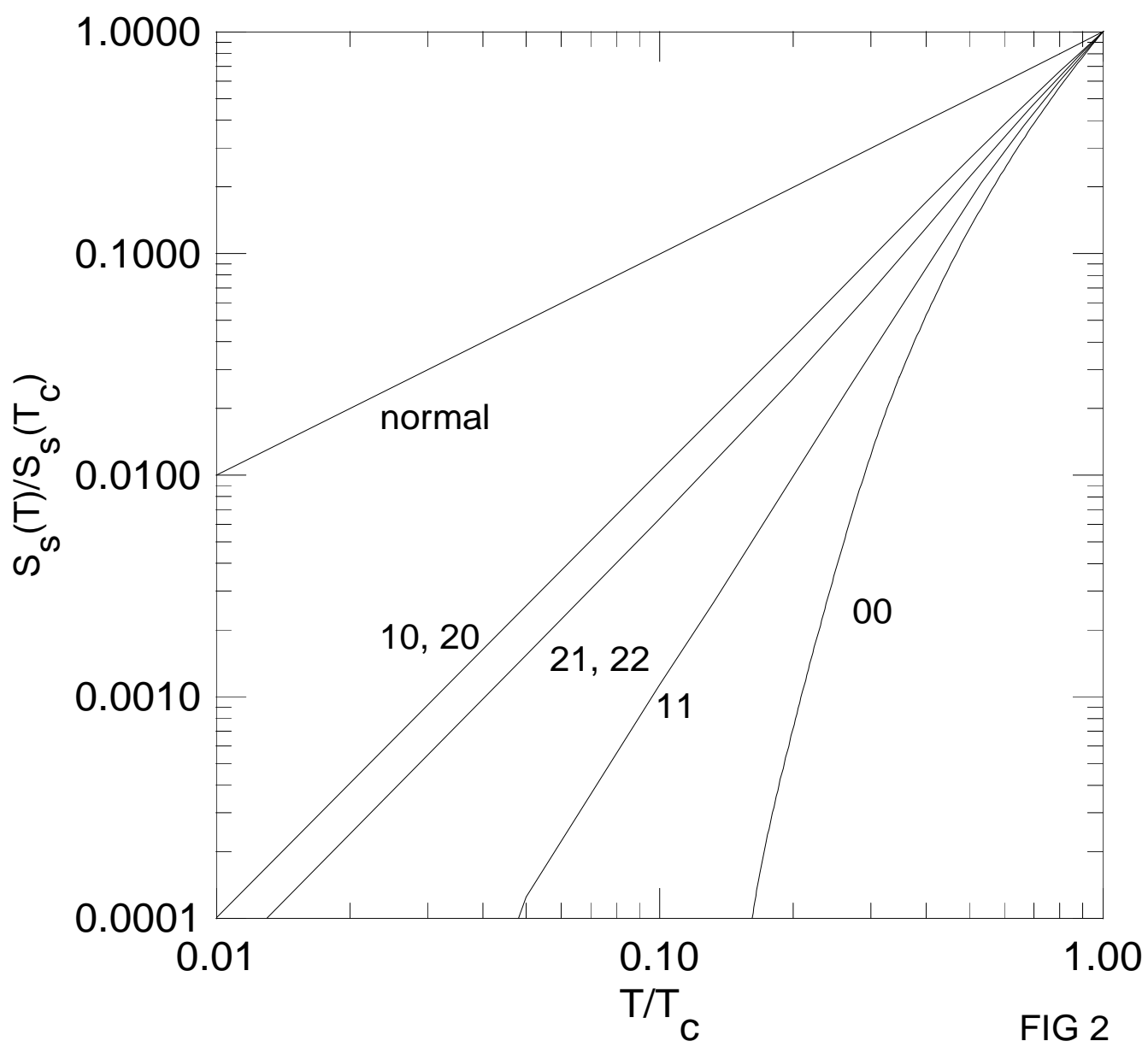


FIG 2

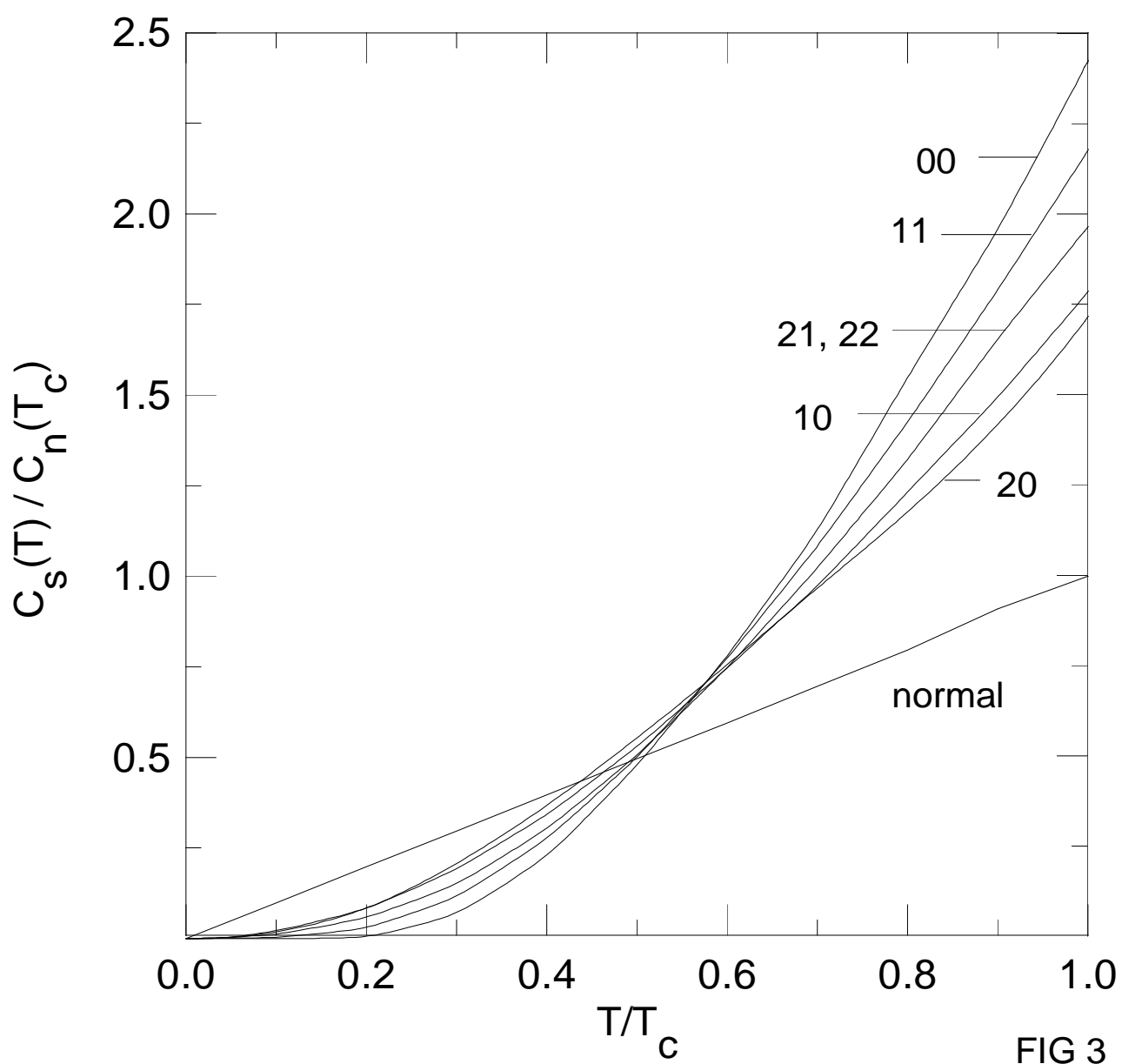


FIG 3

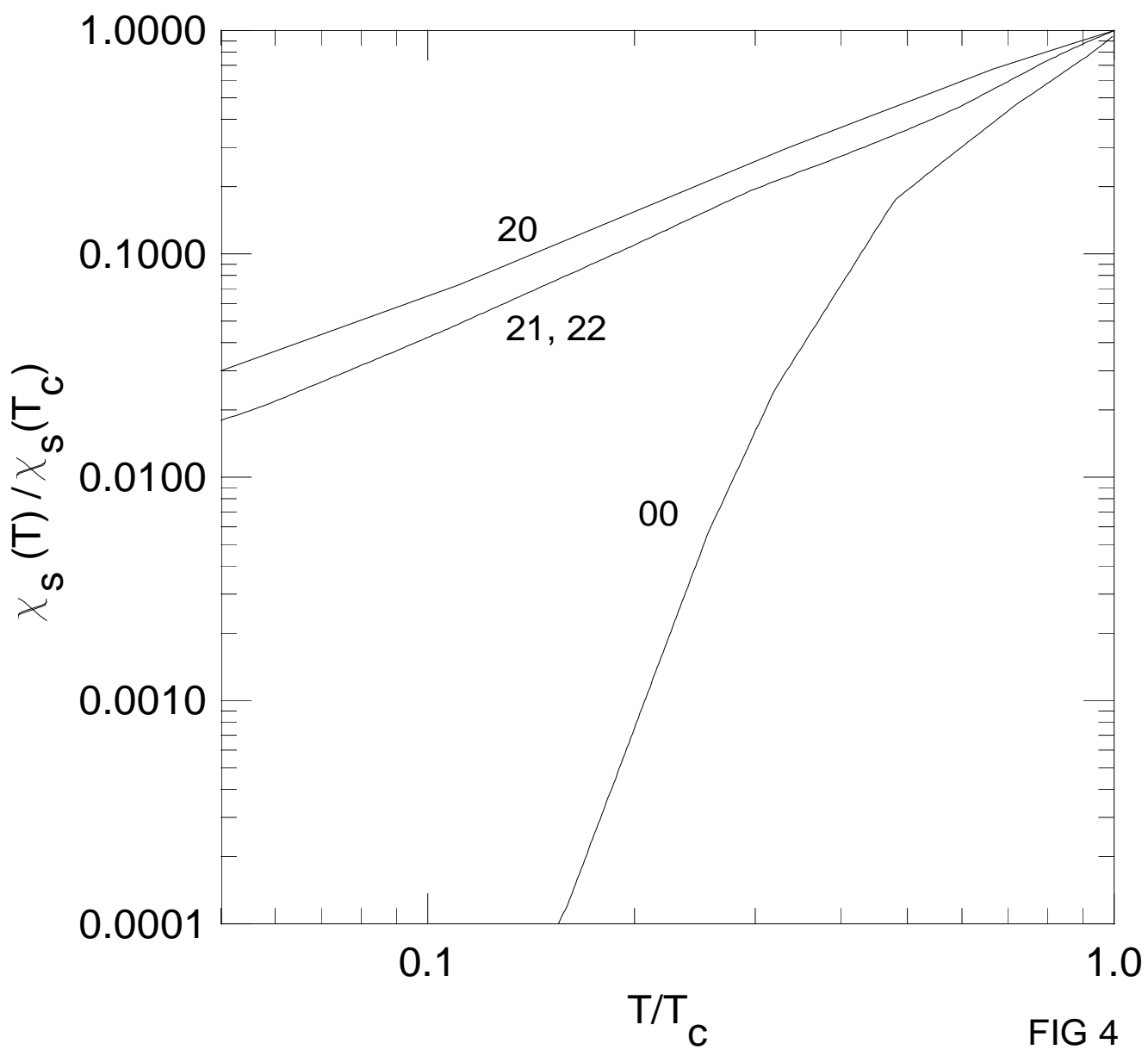


FIG 4

